International Journal of Scientific Reports
Dutta K et al. Int J Sci Rep. 2024 Apr;10(4):102-110
http://www.sci-rep.com
pISSN 2454-2156 | eISSN 2454-2164
DOI: https://dx.doi.org/10.18203/issn.2454-2156.IntJSciRep20240688

Original Research Article

Estimation of thermodynamics properties as a measure of the extent of interference in a conducting polymer based electrochemical aqueous ion sensor

Kusumita Dutta[1,2]*, Siddhartha Panda[1,2]

[1]Department of Chemical Engineering, Indian Institute of Technology Kanpur, Kanpur, Uttar Pradesh, India
[2]National Centre for Flexible Electronics, Indian Institute of Technology Kanpur, Kanpur, Uttar Pradesh, India

Received: 28 February 2024
Revised: 08 March 2024
Accepted: 14 March 2024

***Correspondence:**
Dr. Kusumita Dutta,
E-mail: kusumitasword@gmail.com

ABSTRACT

Background: Interference of other ions towards the target analyte in an electrochemical sensor is typically estimated utilizing the peak reduction (PR) technique and the selectivity coefficient technique, both of which have limitations. In our earlier works, a scale of interference was developed using the barrier width (BW) technique based on Simmon's model utilizing a conducting polymer-based sensor for the detection of Cd^{2+} by square wave voltammetry (SWV). Also, a new scale of interference was generated with higher resolution by incorporating the BW technique along with adsorption isotherms and the PR technique.
Methods: The present work takes the investigation further at the electrode-electrolyte interface to explain the interference effect using thermodynamic parameters such as the partition coefficient, enthalpy and reorganization energy. The length of the reaction site for Cd^{2+} can also measure interference effect. In this work, SWV for Cd^{2+} detection in presence of interfering species at different temperatures were conducted, $-\Delta G_{ad}$ values were extracted and all the thermodynamic parameters were evaluated. The novelty of this work lies in incorporation of these thermodynamic parameters along with BW values (d) to explain the interference phenomena.
Results: The variation of the thermodynamic properties for Cd^{2+} in presence of interfering species were examined. Correlation coefficients were developed from the thermodynamic parameters and the d values to explain the extent of interference.
Conclusions: This study can provide information on the thermodynamic properties which can be predicted from BW technique. The correlation coefficients would help obtain an estimate of the interference with the need of lesser number of experiments.

Keywords: Enthalpy, BW, SWV, Thermodynamics, Reorganization energy

INTRODUCTION

Heavy metal contamination is a potential threat to the environment.[1,2] One such heavy metal ion is cadmium and cadmium toxicity can lead to several health hazards.[3] Cadmium contamination raises from fuel combustion, fertilizers, industrial wastes.[4-8] Selectivity is an important performance parameter for an electrochemical sensor.[9,10] To characterize the selectivity, i.e. extent of interference, two techniques-the PR technique peak or signal reduction technique, and the selectivity coefficient technique are widely used. However, both have limitations. The PR technique requires a large number of experiments and the selectivity coefficient method, which is based on the Nicholsky Eisenmann equation, is not suitable for ions with different charges.[11,12] In our earlier work, a BW technique which incorporates the tunneling mechanism based on Simmon's model used in variety of other

electrochemical works was used for the first time for sensing applications to predict the level of interference of different ions for the detection of an analyte (Cd^{2+}) by SWV in a conducting polymer based electrochemical sensor.[10,13-15] In a subsequent work extent of interference was explained by involving the PR technique, adsorption isotherm and the BW technique.[16] In this work, further investigations at the electrode-electrolyte interface have been undertaken to express the interference effects in terms of various thermodynamic parameters.

Since the present work undertakes further investigation of the mechanism of interference, therefore a brief outline of the work conducted in our earlier works, is presented.[10,16] A schematic of process of detection of Cd^{2+} undertaken with the possible charge transport mechanism is presented in Figure 1.

The conducting polymer coated stainless steel (SS) electrode was used as the working electrode after surface functionalization with iminodiacetate groups which creates a self-assembled monolayer (SAM) on the surface. After preconcentration at open circuit potential, a negative potential of -1.2 V was applied to the electrodes for 200s. Cd^{2+} ions got stripped away from the electrode surface at -0.78 V while varying the potential towards positive direction giving a square wave peak. The interference tests were conducted with different test ions using the PR and the BW techniques and the ions were categorized into four different groups-non-interfering, less, moderately and heavily interfering ions. The BW technique successfully predicted the extent of interference, and a scale of interference was generated requiring lesser number of experiments. In the next work, Cr^{6+} (heavily interfering), Fe^{2+} (moderately interfering) and Al^{3+} (less interfering) ions were selected for further studies.[16] By incorporating the BW technique, the PR technique and the adsorption process, a new scale of interference was generated with higher resolution. Although a higher resolution was obtained, this required a large number of experiments. Moreover, it could not provide complete information of the thermodynamic properties of the system. To overcome this limitation, an attempt is made in the present work to evaluate the thermodynamics parameters of the sensing system.

Various thermodynamic parameters including include partition coefficient, enthalpy, reorganization energy can explain the electrode surface-analyte interaction which gets affected in presence of the interfering species.[17,18] It is also important to obtain the size or length of the reaction site (x) at the electrode surface to capture Cd^{2+} and investigate whether this length is affected by the presence of interfering species. By incorporating the thermodynamic analysis and the BW technique, it is possible to develop some correlation coefficients. The utility of such coefficient is that if only d values are provided then using these coefficients and by doing a handful no of SWV experiments the thermodynamic parameters can be estimated without any further study and vice versa, in presence and absence of interfering ions which is the novelty of this work. Till date, to our knowledge, there is no report where thermodynamic and charge transport parameters were utilized to explain the interference phenomena in an electrochemical sensor. The results obtained in this work can be considered for development of integrated sensor device.

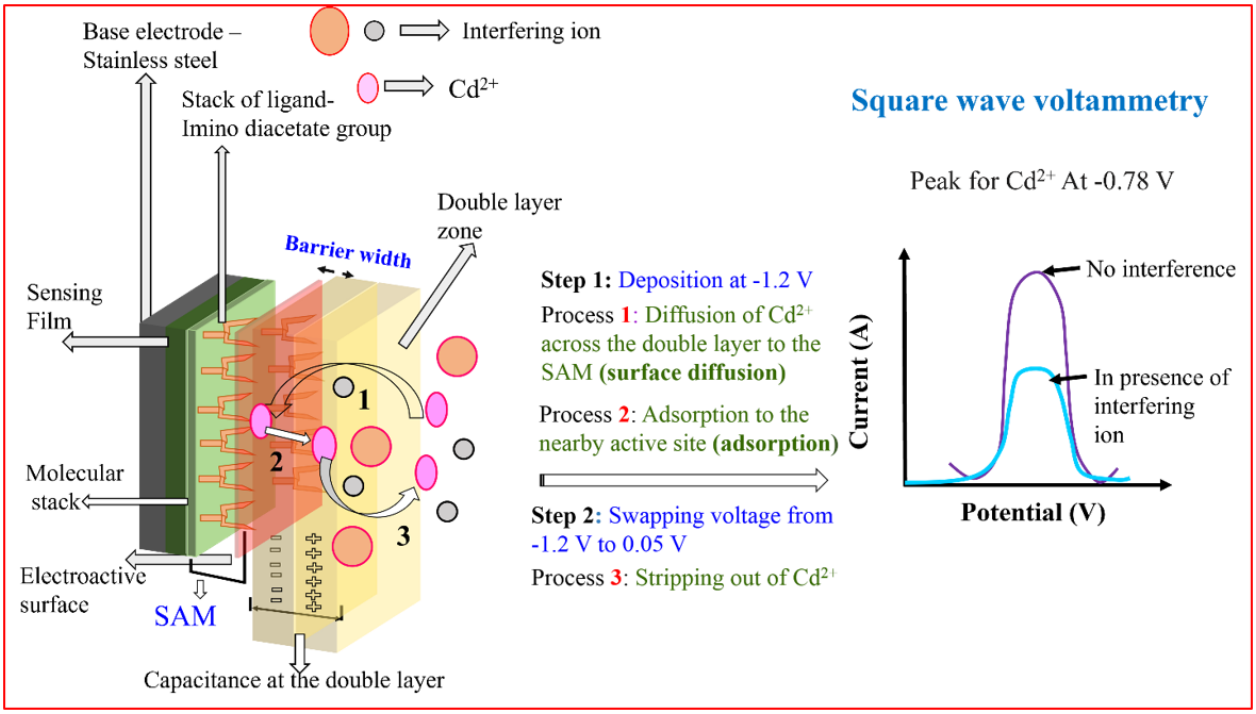

Figure 1: Schematic of the detection process of Cd^{2+} in presence of interfering ions, with possible mechanisms of charge transport.

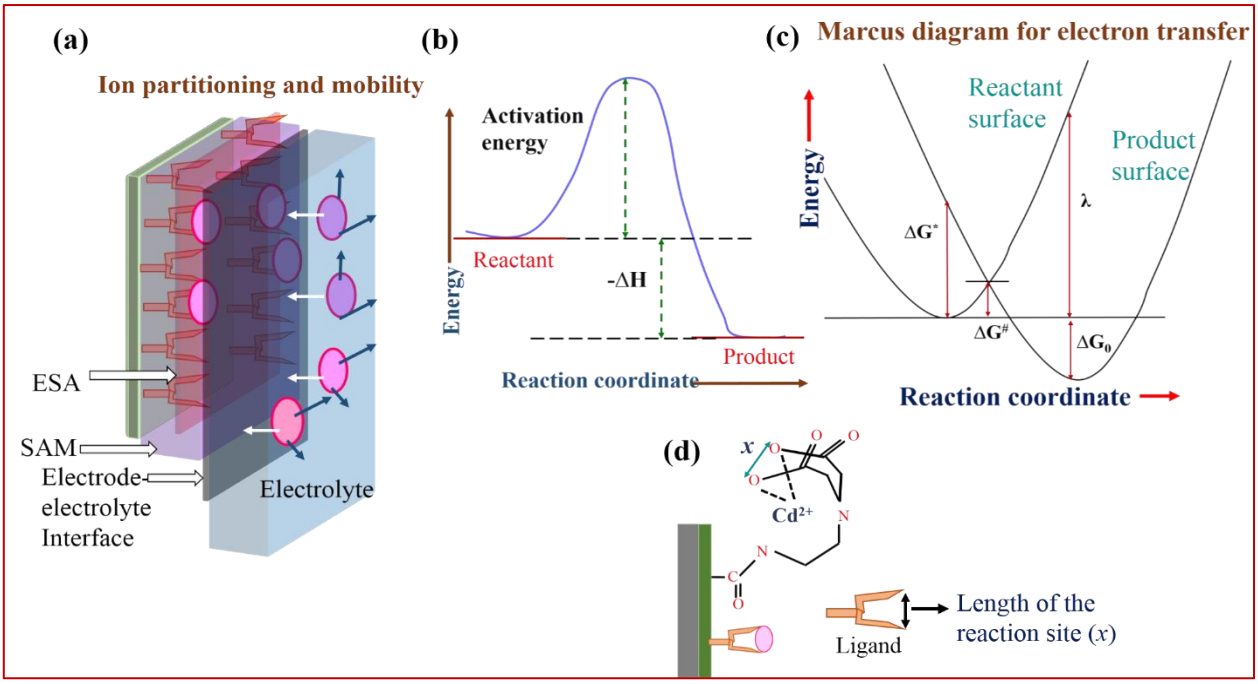

Figure 2: Illustrations of the various thermodynamic factors which influence the charge transport mechanism - (a) ion partitioning, (b) energy diagram showing enthalpy and activation energy to explain the interference effect, (c) Marcus diagram for electron transfer and (d) schematic of the reaction site.[40]

In this work, SWV experiments to detect Cd^{2+} in presence of interfering ions were conducted at different temperature. From the SWV experiments adsorption isotherms were constructed from which the $-\Delta G_{ad}$ values were calculated at different temperatures with different concentrations of interfering ions, Al^{3+} (less-interfering), Fe^{2+} (moderately interfering) and Cr^{6+} (heavily interfering). From these values, thermodynamic parameters, were evaluated. The value of *x* was extracted from the reorganization energy. These factors were used to explain extent of interference and were benchmarked with BW technique performed in our previous works.[10,16] Finally, an attempt was made to establish correlation with these thermodynamic parameters and the *d* values.

METHODS

Experimental

Materials and methods were similar to those reported in one of our published works.[10] For better understanding, a brief description of experimental methods is provided here.

Study period including experiments, analysis, simulation and interpretation for this work was from January 2020 to December 2023. Study place was department of chemical engineering, Indian institute of technology Kanpur.

As reported in our previous work, a copolymer was synthesized from aniline and N-phenylglycine by chronopotentiometry onto the SS 304 electrode and surface-functionalized with iminodiacetate groups.[10] The protocols are mentioned in the previous work.[10] In the present work, for the less interfering, moderately interfering and highly interfering categories, Al^{3+}, Fe^{2+} and Cr^{6+} were chosen, respectively as mentioned in our earlier work, and experiments were performed.[10]

Experimental design

The complete procedure is mentioned in experimental section of one of our previous work where the experiments were carried out at 298 K.[10] In the present work the same experiments were conducted at different temperatures: 288 K, 308K and 318 K. The temperature range for this work was chosen from 288 K to 318 K, as beyond this range, the LOD was found to be higher than 50 ppb in absence of interfering ions. Adsorption isotherms were constructed as in the earlier works (not shown here), and the corresponding values of $-\Delta G_{ad}$ were evaluated.[10,16] The complete procedure is described in brief as follows. As described in our earlier work, three concentrations: 100 ppb, 1 and 10 ppm of Cd^{2+} were selected. A pictorial description of interfering behavior of these test ions is depicted in our earlier publication where the terms 'h' and 'C_{hR}' are explained.[9] C_{hR} was the highest value of the test ion and ~0.001 C_{hR} was the specific concentration of the interfering ions at which no interference was observed, i.e., decrease in 'h' was not observed. To quantify the interference behavior, 2 extreme values, (C_{hR}) and (0.005 C_{hR}), were selected for further studies which were of different values for different types of test ions. Table 1 shows concentrations for Al^{3+}, Fe^{2+} and Cr^{6+} used in present work.

Table 1: Concentrations of the interfering ions.

Interfering ion	Concentrations
Al^{3+}	100 ppm, 10 ppm, 5 ppm
Fe^{2+}	10 ppm, 5 ppm, 1 ppb, 500 ppb
Cr^{6+}	100 ppb, 10 ppb, 1 ppb, 500 ppt

Experiments utilizing SWV were conducted for different concentrations of Cd^{2+} in presence of interfering ion with the concentration as mentioned illustrated in Table 1. Electrolyte was bicomponent solution which comprised of Cd^{2+} and the interfering ion in 0.1 M phosphate buffer solution at pH 3.3, 0.1 M of phosphate buffer of 100 ml was prepared from 0.1 M di-sodium-hydrogen-phosphate solution. Upon gradual addition of 0.1 M solution of hydrochloric acid pH 3.3 was obtained.

Square wave voltammetry

As mentioned, the SWV experiments were conducted for Cd^{2+} with different concentrations of the interfering species as mentioned in Table 1 at a single temperature of 298 K, reported in our earlier work.[10] In the present work the same experiments were conducted at 288K, 308 K and 318 K. The electrode surface functionalized with IDA was dipped in the electrolyte for about 30 min without application of any external potential. A potential of -1.2 V was supplied to the working electrode for approximately 200 s to deposit the ions at the electrode surface. Next, the potential was transposed towards the higher values with a square wave pulse and Cd^{2+} got stripped out of the surface at -0.78 V. For all SWV tests, amplitude of 0.1 V, step potential of 0.075 V, frequency of 25 Hz was maintained. From the SWV plots, the peak currents were evaluated, and the adsorption isotherms were constructed from which the $-\Delta G_{ad}$ values were evaluated. From the $-\Delta G_{ad}$ values obtained at different temperatures, the $-\Delta H$ values were evaluated.

RESULTS

The variations of P, ΔH, $-\lambda$ and x for Cd^{2+} in presence of different concentrations of different interfering ions are described below.

Partition coefficient

In our previous work, the $-\Delta G_{ad}$ values for Cd^{2+} were calculated in the presence of interfering ions at different concentrations.[16] The $-\Delta G_{ad}$ value for Cd^{2+} in absence of any interfering ion was 49.53 kJ/mol as reported in our previous work.[10] From ΔG_{ad} values, partition coefficients were calculated using the following equation (1),

$$\Delta G = -RT \ln P \ldots\ldots (1)^{19}$$

where P signifies partition coefficient, R denotes the universal gas constant. and T is the temperature. The ln P values obtained from equation (7) were plotted against p[Interfering ion] (i.e. $p[Al^{3+}]$, $p[Fe^{2+}]$ and $p[Cr^{6+}]$) and are shown in Figure 3. p[Ion] can be defined as $-\log_{10}[C_{ion}]$. C_{ion} is the concentration of that ion.

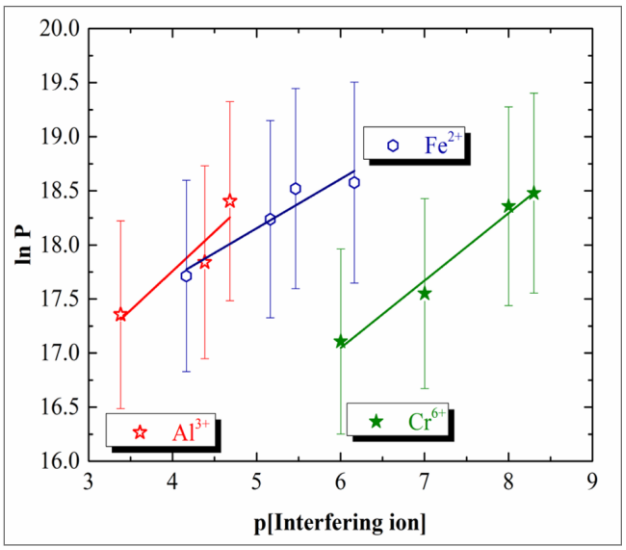

Figure 3: Variation of ln P with respect to p[Interfering ion] ($p[Al^{3+}]$, $p[Fe^{2+}]$, $p[Cr^{6+}]$).

From these plots, the slopes (termed here as S_{PC}) with respect to $p[Al^{3+}]$, $p[Fe^{2+}]$ and $p[Cr^{6+}]$ were calculated and are listed in Table 2.

Table 2: Values of κ_{BW}, S_{PC}, S_{λ} and S_{H}.

Interfering ion	κ_{BW} (Å/p[Cd] p[Interfering ion])[16]	S_{PC} ([p[Interfering ion]]$^{-1}$)	S_H (kJ/mol p[Interfering ion])	S_λ (kJ/mol p[Interfering ion])	S_X (Å/ p[Interfering ion])
Al^{3+}	0.113	0.712	2.14	0.129	0.433
Fe^{2+}	0.123	0.523	2.87	0.092	1.659
Cr^{6+}	0.142	0.572	2.83	0.112	0.533

Enthalpy

Partition coefficient P can be considered as equilibrium constant and can evaluated using Van't Hoff equation.[20]

$$\Delta G = 2.303 \log P \ldots\ldots (3)^{21,22}$$

Where, ΔG is the Gibb's free energy.[21]

To calculate the -ΔH values, Van't Hoff's isochore can be used as shown in equation (4)

$$\Delta G = 2.303 \frac{\Delta H}{RT} + \varphi \quad \ldots\ldots(4)^{23}$$

where φ is a constant. This method stands with the assumption that the ion partitioning is constant over the range of temperature used.[23]

The $-\Delta G_{ad}$ values obtained at different temperatures were put into equation (3) to calculate log P. Further, the plots of (1000/T) vs log P for Cd^{2+} for the interference effects from Al^{3+}, Fe^{2+} and Cr^{6+} provided the -ΔH values in presence of different concentrations of these test ions. From these plots of -ΔH vs p[Interfering ion], the slopes S_H values were evaluated and plotted against p[Al^{3+}], p[Fe^{2+}] and p[Cr^{6+}] as shown in Figure 4.

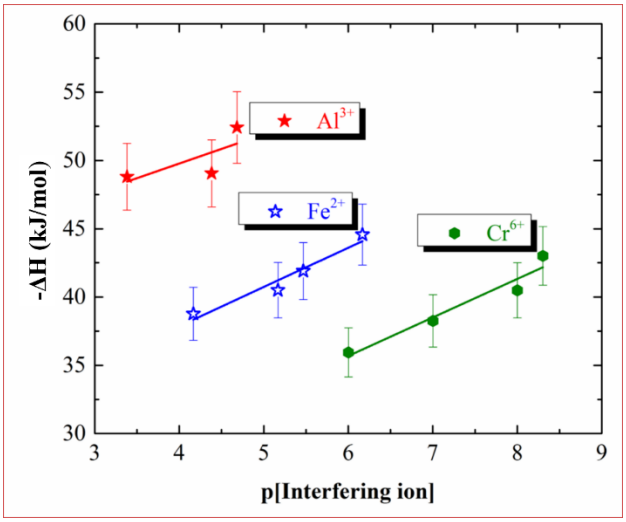

Figure 4: Variation of -ΔH with respect to p[Interfering ion] (p[Al^{3+}], p[Fe^{2+}], p[Cr^{6+}]).

Reorganization energy and length of reaction site (x)

The energy associated with the activated state is given by,

$$\Delta G^{\#} = \frac{(\Delta G^0 + \lambda)^2}{4\lambda} \ldots\ldots\ldots\ldots(6)^{24}$$

Where, $\Delta G^{\#}$ represents free energy of activated state and is regarded as reaction barrier and ΔG^0 is standard Gibb's free energy. In this work, concept of reorganization energy was used to explain interference phenomena.[24]

An analytical approach was taken based on the experimental data, assuming the values of ΔG_{ad} in presence of the interfering ion as the $\Delta G^{\#}$ i.e., the free energy of activated state indicating the reaction process overcoming the interference of the several test ions. In order to calculate ΔG^0, the following equation was used,

$$\Delta G^0 = -nFE^0 \ldots\ldots\ldots(7)^{25}$$

where n is number of electrons transferred, F is Faraday's constant and E^0 is standard electrode potential. Equation (6) was solved in simplified format using Matlab.

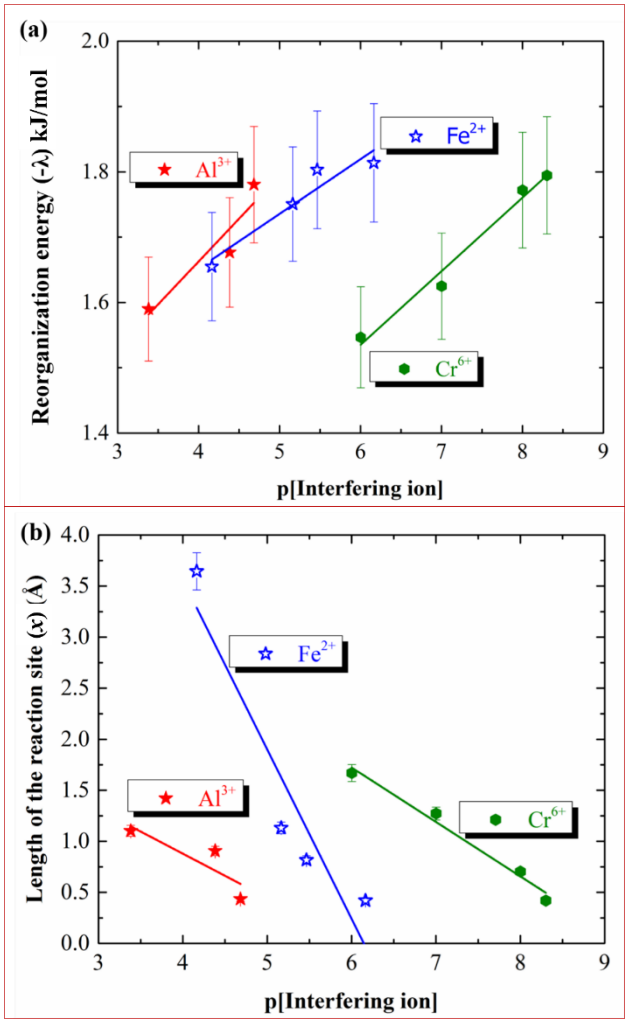

Figure 5: Variation of (a) reorganization energy (-λ) kJ/mol and (b) length of the reaction site (x) for 100 ppb of Cd^{2+} with respect to p[Interfering ion] (p[Al^{3+}], p[Fe^{2+}], p[Cr^{6+}]).

From equation (6), the values of -λ were plotted against p[Interfering ion] (p[Al^{3+}], p[Fe^{2+}] and p[Cr^{6+}]) and are shown in Figure 5 (a). From the plots, the slopes (S_λ) with respect to p[Al^{3+}], p[Fe^{2+}] and p[Cr^{6+}] were calculated and listed in Table 2. The value of -λ for Cd^{2+} in absence of interfering ions was 2.087 kJ/mol. While calculating the -λ values from equation (6), two values of -λ were obtained (as it is a quadratic equation), and the minimum amount of energy was considered.

The -λ value, obtained from equation (1), was used to calculate the length of the reaction site (x) for Cd^{2+} as a measure of the interference effects using equation (7).[14,16]

$$\lambda = e^2\left(\frac{1}{\epsilon_0} - \frac{1}{\epsilon_S}\right)\left(\frac{1}{2r_1} + \frac{1}{2r_2} - \frac{1}{r_d}\right) \ldots.(7)$$

where, e is the charge transferred, ε_0 is the relative permittivity of the vacuum, ε_S is the dielectric constant of solvent, $2r_1$ is assumed to be the length (x) of the reaction site at the SAM where the Cd^{2+} get adsorbed, r_2 is the solvated ionic radius of Cd^{2+} and r_d is considered as the d values as evaluated in our previous works.[10,16] Since, the concentration of Cd^{2+} in electrolyte is very low, i.e. ~100 ppb, therefore, dielectric constant of water is chosen.

To calculate the length of the reaction site (x), equation (7) was used and the values were plotted against $p[Al^{3+}]$, $p[Fe^{2+}]$ and $p[Cr^{6+}]$ as shown in Figure 5 (b). The length of the reaction site (x) for 100 ppb concentration of Cd^{2+} was 0.4191 Å in absence of interfering ions. As reported, the crystal ionic radius, stokes and hydrated ionic radius for Cd^{2+} was 0.97, 3.41 and 2.63 Å.[27] In several works, the authors have considered the above reported values for their works. In this work the solvated ionic radius for Cd^{2+} was taken to be 2.63 Å. To the best of our awareness, till date there is no report till date where x for Cd^{2+} was calculated using the Marcus theory of electron transfer incorporating the BW as the distance between the analyte and sensing surface.

DISCUSSION

Partition coefficient

In our previous work, the $-\Delta G_{ad}$ values for Cd^{2+} were calculated in the presence of interfering ions at different concentrations.[16] It was seen that with increase in the concentrations of the test ions, the $-\Delta G_{ad}$ values decreased, predicting comparatively weaker interactions between the electrode and the target analyte. For each of the cases, the values were found to be more than 40 kJ/mol which indicates chemisorption.[28,29] In our earlier works, it was evident that higher the adsorption lower was the limit of detection.[4,10,16] The process of adsorption is accompanied by partitioning of ions i.e., distribution of ions among the electrode surface and electrolyte.[30] Figure 2(a) shows a pictorial representation of ion partitioning between electrode surface and electrolyte. Effect of interference on partition coefficient of the desired analyte was investigated for adsorption of benzene (desired analyte) in presence of interferents such as n-butanol, o-xylene, n-pentane in Tenax-GC system, however, for electrochemical sensors concept of dependency of partition coefficient on interferants is employed here for first time to predict extent of interference.[30,31]

It was seen from Figure 3 that with decrease in the concentration of the interfering ions, the values of ln P increase. As mentioned earlier, partition coefficient is a measure of the distribution of ions between the electrode and the electrolyte. Therefore, it is evident that with increase in interfering species concentration, less number of Cd^{2+} ions get adsorbed into the active site of the electroactive surface.

In our previous work, the plots of the d values of Cd^{2+} in presence of varying interfering ion concentrations against p[Cd] are illustrated in Figure 4 of that work.[16] The d values showed a decreasing trend with decrease in interfering ion concentrations. The values of the slopes (S_{BW}) were evaluated and plotted S_{BW} against p[Interfering ion] was shown in 'Figure 5' of that work.[16] From the plots of p[Interfering ion] vs S_{BW}, slopes (κ_{BW}) were calculated and are listed in Table 2.[16] The above analyses based on partition coefficient and d shows that increase in ln P is accompanied by decrease in d. Higher the interference lesser number of Cd^{2+} ions will be adsorbed at electrode. Similarly, higher the interference, the charge has to cover more distance to tunnel through, resulting in a higher value of d. Therefore, there could be some interrelation between the partitioning of ions and d values. To find this out, a simple simulation was carried out by using the values of S_{PC} and κ_{BW} in different sets of equations, and a following correlation coefficient a, with units of Å/p[Cd](p[Interfering ion])^2, is proposed where

$$a = (\kappa_{BW})(S_{PC}) \ldots\ldots (2)$$

The value of a is almost constant and lies in the range ~0.065 to 0.08.

Enthalpy

The thermodynamic properties can be used to understand the charge transport mechanism simultaneously can predict the extent of interference. As shown in Figure 2 (b), activation energy is needed for a reaction to occur. The total energy required for the reaction includes enthalpy, ΔH, of the reaction.[33] In absence of any barrier as well as interference effect, the energy required is lower as compared to that in presence of the interference effect. This concept is based on catalysis-in presence of catalysts, the total energy requirement is lower than that in absence of catalysts.[34]

From the Figure 4, it was obvious that the $-\Delta H$ values were increasing with decrease in interfering ion concentrations. As from the Figure 2 (b), it can be understood that with decrease in $-\Delta H$, more energy would be needed in order to bring about a successful reaction. From the plots of p[Interfering ion] vs $-\Delta H$, the slopes S_H values were evaluated as well as are mentioned in the Table 2.

It can be observed that, increase in $-\Delta H$ was accompanied by decrease in values of d. Higher the interference, lower was the value of $-\Delta H$, and higher was the value of d. Therefore, there may be some interrelation between the enthalpy and the BW of electron transfer. To investigate this, a simple simulation was carried out by fitting the values of S_H and κ_{BW} in different sets of equations and a following correlation coefficient b (Å kJ/mol p[Cd] (p[Interfering ion])^2) was obtained which is described in equation (5),

$b = (\log S_H)(\kappa_{BW})$…….(5)

The value of b is almost constant and varies between 0.035-0.065. Higher the interference, higher will be the value of the coefficient b.

Reorganization energy and length of reaction site (x)

As reported, the SAM modified electrodes gained interests in studying the long-range transfer of electron between the electrodes and redox active molecules.[35,36] According to Marcus theory of electron transfer, rate constant of electron transfer depends on the free energy barrier which in turn depends on the reorganization energy.[37] The reorganization energy can be defined as the energy required for deforming the nuclear configuration from the donor to the acceptor state without any transfer of electrons.[38,39] It may be evaluated by designing a model in which there is rapid transfer of electrons to the acceptor state so that there is no change in the nuclear configuration in the donor state and following to this, there is a change in the nuclear configuration of the acceptor state. This change in free energy correspond to -λ. This design strategy was defined by Sharp and was followed in this work.[40] Figure 2 (c and d) shows the Marcus diagram of the electron transfer and the schematic of the reaction site.

It was seen from Figure 5 (a) that with decrease in interfering ion concentration, the values of -λ decrease. In all the cases, the values of -λ for Cd^{2+} in presence of interfering ions were less than that in absence of interfering species. For all cases in presence of interfering ions, the length of the reaction site (*x*) for Cd^{2+} was higher than that in absence of any interfering species. It was observed that with increase in concentration of the interfering species, the values of the length of the reaction site (*x*) for Cd^{2+} decreased. This indicates that other solvated ions occupy the space at the electrode-electrolyte interface which increases the length of the reaction site (*x*) for Cd^{2+}. From Figure 5 (b) the slopes (S_R) for each of the cases of interference were extracted, and were 0.433, 1.659 and 0.533 Å/p[Interfering ion] for Al^{3+}, Fe^{2+} and Cr^{6+}, respectively. Again, it is pertinent to mention here that in this work an attempt has been made to explore the mechanism of the interference phenomena with the help of the concept of the reorganization energy, based on the Marcus electron transfer theory, with the assumptions configured depending on the experimental conditions.

The *d* values for 100 ppb of Cd^{2+} in presence of interfering ions were mentioned in our previous work.[16] Based on the analyses incorporating (-λ) and the *d* values, it was obvious that decrease in -λ was accompanied by increase in the *d* values. Higher the interference, lower is the energy necessary for the distortion of the nuclear configuration from reactant to product indicating lesser interaction between the electrode surface and Cd^{2+}. Similarly, higher the interference, higher is the value of *d*. Therefore, there may be some interrelation between the reorganization energy and the BW of electron transfer. In order to investigate further, a simulation was carried out by putting the values of S_λ and κ_{BW} in different sets of equations and a following correlation coefficient *c* was achieved as shown in equation (8).

$c = \kappa_{BW} S_\lambda$……. (8)

The value of *c* (with the unit Å kJ/mol p[Cd] (p[Interfering ion])^2) is almost constant and lies in the range ~0.012-0.016.

Analysis based on correlation coefficients

From the above analyses, it is evident that the correlation coefficients a, b, c can be used to explain the interference effects of several ions towards Cd^{2+}. Using these coefficients and the *d* values, with limited number of experiments, information about the interference effects which can explain the fundamental mechanisms for sensing can be gathered. Similarly, if $-\Delta G_{ad}$ values are known then the other thermodynamic properties can be estimated, and using the correlation equations, values of the *d* can be predicted in presence or absence of interfering ions. These correlation coefficients can be used for the design and testing of specific molecules and the electrode-electrolyte interactions so that better sensing or better performance for a sensor or any other processes can be achieved.

Limitations

The correlation coefficients obtained from this work are limited for this specific sensor i.e., conducting polymer synthesized from aniline and N-phenylglycine based Cd^{2+} sensor only. For a different sensor, a similar study should be conducted and new correlation coefficients should be generated. The analytical study is tedious but once the correlation coefficients are generated these minimize the efforts.

CONCLUSION

In this work, three interfering ions Cr^{6+} (heavily interfering), Fe^{2+} (moderately interfering) and Al^{3+} (less interfering) ions were used. The partition coefficient for Cd^{2+} was calculated from the $-\Delta G_{ad}$ values for Cd^{2+} in presence and absence of interfering ions. Then the enthalpy and reorganization energy values were evaluated. From the λ values, the lengths of the reaction sites (*x*) for Cd^{2+} were calculated. From the plots of ln P, -ΔH, -λ and x against p[Interfering ion], the slopes S_{PC}, S_H S_λ and S_X, respectively, were extracted respectively. It was observed that ln P and -ΔH values showed a decreasing trend with increase in interference while the reorganization energy as well as the length of the reaction site showed an increasing trend. As mentioned in our previous work, for each concentration of Al^{3+}, Fe^{2+} and Cr^{6+}, the slopes S_{BW} were evaluated, plotted against p[Interfering ion], from which slopes κ_{BW} values were

extracted. Correlation coefficients a, b and c were evaluated from S_λ and κ_{BW}, from S_H and κ_{BW}, S_λ and from κ_{BW} values, respectively. The values of a, b and c were almost constant and lie in the ranges 0.065-0.08, 0.035-0.065 and ~0.012 to 0.016, respectively. A highlight of this work is that *d* values along with correlation coefficients are sufficient to explain interference phenomena as well as various thermodynamic parameters such as enthalpy, partition coefficient, reorganization energy without performing SWV experiments as well as constructing adsorption isotherms. Similarly, if thermodynamic parameters are provided along with the correlation coefficients, charge transport parameter *d* can be evaluated without performing the BW analysis. Utility of the correlation coefficients lies in the fact that by doing limited analysis, several information related to transport and sensing could be obtained. These coefficients can be used for design of materials and processes.

Funding: Ministry of Electronics and Information Technology (MEITY), India
Conflict of interest: None declared
Ethical approval: Not required

REFERENCES

1. Ho CK, Robinson A, Miller D, Davis M. Overview of Sensors and Needs for Environmental Monitoring. Sens. 2005;5(1);4-37.
2. Liu W, Liu Y, Yuan Z, Lu C. Recent Advances in the Detection and Removal of Heavy Metal Ions Using Functionalized Layered Double Hydroxides: A Review. Indus Chemi Mat. 2023;1(1):79-92.
3. Moon S, Lee J, Yu JM, Choi H, Choi S, Park J, et al. Association between Environmental Cadmium Exposure and Increased Mortality in the U.S. National Health and Nutrition Examination Survey (1999-2018). J Expo Sci Environ Epidemiol. 2023;33(6):874-82.
4. Dutta K, Panda S. Thermodynamic and Charge Transport Studies for the Detection of Heavy Metal Ions in Electrochemical Sensors Using a Composite Film of Aniline, N-Phenylglycine and Graphene Oxide. J Electrochem Soc. 2019;166(14):B335-42.
5. Jiang K, Xing R, Luo Z, Huang W, Yi F, Men Y, et al. Pollutant Emissions from Biomass Burning: A Review on Emission Characteristics, Environmental Impacts, and Research Perspectives. Particuology. 2024;85:296-309.
6. Samrane K, Latifi, M, Khajouei M, Bouhaouss A. Comprehensive Analysis and Relevant Developments of Cadmium Removal Technologies in Fertilizers Industry. Miner Eng. 2023;201:108189.
7. Mashhadikhan S, Ebadi Amooghin A, Sanaeepur H, Shirazi MMA. A Critical Review on Cadmium Recovery from Wastewater towards Environmental Sustainability. Desalination. 2022;535:115815.
8. Gajanayake GKUP, De Silva DSM, Atapattu HYR. Cadmium Extraction from the Electrodeposition Waste Generated in CdS/CdTe Solar Cell Fabrication. J of Mat Sci: Mat in Electronics. 2023;34(12):1071.
9. Li S, Zhang C, Wang S, Liu Q, Feng H, Ma X, Guo J. Electrochemical Microfluidics Techniques for Heavy Metal Ion Detection. Analyst. 2018;143(18):4230-46.
10. Dutta K, Panda S. Identification of the Levels of Interference of Ions toward Heavy Metal Detection in Electrochemical Sensors Using the Barrier Width Technique. J Electrochem Soc. 2018;165 (9): B378-85.
11. Umezawa Y, Bühlmann P, Umezawa K, Tohda K, Amemiya S. Potentiometric Selectivity Coefficients of Ion-Selective Electrodes. Part I. Inorganic Cations (Technical Report). Pure and Applied Chemistry. 2000;72(10):1851-2082.
12. Bakker E. Determination of Unbiased Selectivity Coefficients of Neutral Carrier-Based Cation-Selective Electrodes. Anal Chem. 1997;69(6):1061-9.
13. Vilan A. Analyzing Molecular Current-Voltage Characteristics with the Simmons Tunneling Model: Scaling and Linearization. The J of Phys Chem C. 2007;111(11):4431-44.
14. Hill CM, Kim J, Bodappa N, Bard AJ. Electrochemical Nonadiabatic Electron Transfer via Tunneling to Solution Species through Thin Insulating Films. J Am Chem Soc. 2017;139(17):6114-9.
15. Hill CM, Kim J, Bard AJ. Electrochemistry at a Metal Nanoparticle on a Tunneling Film: A Steady-State Model of Current Densities at a Tunneling Ultramicroelectrode. J Am Chem Soc. 2015;137(35):11321-6.
16. Dutta K, Panda S. Interference Analysis for Electrochemical Heavy Metal Ion Sensors in Terms of Stripping Current, Barrier Width and Adsorption. J Electrochem Soc. 2018;165(13):B644-50.
17. Madawala H, Sabaragamuwe SG, Elangovan S, Kim J. *In Situ* Measuring Partition Coefficient at Intact Nanoemulsions: A New Application of Single-Entity Electrochemistry. Anal Chem. 2021;93(2):1154-60.
18. Matyushov DV. Reorganization Energy of Electron Transfer. Phys Chem Chem Phys. 2023;25(11):7589-610.
19. Dutra LMU, Ribeiro MENP, Cavalcante IM, Brito DHA; Semião L, Silva RF, et al. Binary Mixture Micellar Systems of F127 and P123 for Griseofulvin Solubilisation. Polímeros. 2015;25(5):433-9.
20. Mashhaditafreshi S, Haghtalab A. Study on Drug Separation in Two-Phase Aqueous Systems Using Deep Eutectic Solvent Consisting of Choline Chloride and 1, 2 Propanediol. J Mol Liq. 2024;393:123603.
21. Raynie DE. Practical Understanding of Partition Coefficients. LCGC North Am. 2023;36(7):275-9.
22. Iqbal M, Tao Y, Xie S, Zhu Y, Chen D, Wang X, et al. Aqueous Two-Phase System (ATPS): An Overview and Advances in Its Applications. Biol Proced Online. 2016;18(1):1-18.
23. Dearden J, Bresnen G. Thermodynamics of Water-Octanol and Water-Cyclohexane Partitioning of

Some Aromatic Compounds. Int J Mol Sci. 2005;6(1):119-29.
24. Houchins G, Pande V, Viswanathan V. Mechanism for Singlet Oxygen Production in Li-Ion and Metal-Air Batteries. ACS Energy Lett. 2020;5(6):1893-9.
25. Bard AJ, Faulkner LR, Leddy J, Zoski CG. Electrochemical Methods: Fundamentals and Applications; John Wiley and Sons: New York, NY. 1980:2:206-356.
26. Hsu CP. Reorganization Energies and Spectral Densities for Electron Transfer Problems in Charge Transport Materials. Phys Chem Chem Phys. 2020;22(38):21630-41.
27. Nightingale ER. Phenomenological Theory of Ion Solvation. Effective Radii of Hydrated Ions. J Phys Chem. 1959;63(9):1381-7.
28. Horsfall MJ, Ayebaemi IS, Augustine A. Studies on the Influence of Mercaptoacetic Acid (MAA) Modification of Cassava (Manihot Sculenta Cranz) Waste Biomass on the Adsorption of Cu^{2+} and Cd^{2+} from Aqueous Solution. Bull Korean Chem Soc. 2004;25(7):969976.
29. Kumar PS, Ramakrishnan K, Kirupha SD, Sivanesan S. Thermodynamic and Kinetic Studies of Cadmium Adsorption from Aqueous Solution onto Rice Husk. Braz J Chemical Eng. 2010;27(2):347-55.
30. Johanson G. Modeling of Disposition. In Comprehensive Toxicology. Elsevier. 2010;1:153-77.
31. Vejrosta J, Roth M, Novák J. Interference Effects in Trapping Trace Components from Gases on Chromatographic Sorbents. J Chromatogr A. 1983;265:215-21.
32. Vejrosta J, Mikešová M, Novák J. Interference Effects in Trapping Trace Components from Gases on Tenax-GC. J Chromatogr A. 1986;354:59-64.
33. Ghaffari F, Khorsandi M, Shekaari H, Zafarani-Moattar MT. Liquid-Liquid Equilibrium Measurements and Computational Study of Salt–Polymer Aqueous Two Phase System for Extraction of Analgesic Drugs. Sci Rep. 2022;12(1):13848.
34. Papamichael EM, Stamatis H, Stergiou PY, Foukis A, Gkini OA. Enzyme Kinetics and Modeling of Enzymatic Systems. In Advances in Enzyme Technology. Elsevier. 2019;71-104.
35. Eckermann AL, Feld DJ, Shaw JA, Meade TJ. Electrochemistry of Redox-Active Self-Assembled Monolayers. Coord Chem Rev. 2010;254(15-16):1769-802.
36. Marcus RA. Tight-binding Approximation for Semi-infinite Solids. Application of a Transform Method and of Delta Function Normalization. J Chem Phys. 1993;98(7):5604-11.
37. Rudolph AM. Chemical and Electrochemical Electron-Transfer Theory. Annu Rev Phys Chem. 1964;15(1):155-96.
38. Mehra R, Kepp KP. Contribution of Substrate Reorganization Energies of Electron Transfer to Laccase Activity. Phys Chem Chem Phys. 2019;21(28):15805-14.
39. Wei YC, Wang SF, Hu Y, Liao LS, Chen DG, Chang KH, et al. Overcoming the Energy Gap Law in Near-Infrared OLEDs by Exciton-Vibration Decoupling. Nat Photonics. 2020;14(9):570-77.
40. Sharp KA. Calculation of Electron Transfer Reorganization Energies Using the Finite Difference Poisson-Boltzmann Model. Biophys J. 1998;74(3):1241-50.

Cite this article as: Dutta K, Panda S. Estimation of thermodynamics properties as a measure of the extent of interference in a conducting polymer based electrochemical aqueous ion sensor. Int J Sci Rep 2024;10(4):102-10.